Improving Of Is-Cfar Using Wavelet De-Noising For Smoothing The Noise In Reference Cells

Asst. Lecturer. Hadi jameel Hadi
Al - Mustafa University College
Technical Computer Engineering Department

Asst. Prof. Dr. Waleed Khalid Abed Ali
AL-Mustansiriya University
College of Engineering Electrical Engineering Department

Abstract :

Constant false alarm rate (CFAR) algorithms allow RADAR systems to set detection thresholds and isolated the target from noise or clutter to keeping the false alarm rate at certain level. In this paper a technique added to Improved Switching IS-CFAR system is used to reduce the non-homogenous effect and clutter wall, this technique is called wavelet de-noising. The detection performance of Improving IS-CFAR using wavelet de-noising (I^2S-CFAR) processor is compared with the IS-CFAR detectors for homogeneous, non-homogenous and clutter wall. By using wavelet de-noising a gain in signal to noise ratio (SNR) about 2.6dB achieved for the same probability of detection.

Keywords: Wavelet Shrinkage, IS-CFAR, reference cells, cell under test (CUT), I^2S-CFAR

"تحسين مُعالج نسبة الإنذار الكاذب الثابت الأبدالي المُحسن بواسطة طريقة تقليص المويجة لتقليل الضوضاء في الخلايا الأساسية"

ا.م.د. وليد خالد عبد علي
الجامعة المستنصرية
كلية الهندسة قسم الهندسة الكهربائية

م.م. هادي جميل هادي
كلية المصطفى الجامعة
قسم هندسة تقنيات الحاسبات

الخلاصة

تَسْمحُ خوارزمياتُ نسبةِ الإنذار الكاذبِ الثابتة لأنظمةِ الرادار لوَضْع عتباتِ الكشفِ وعَزل الهدفَ مِنْ الضوضاءِ أَو الإشارة غير المرغوب بها لإبقاء نسبة الإنذار الكاذب في مستوى محدد. في هذا البحث تم إضافة تقنية إلى نسبة الإنذار الكاذبِ الثابتةِ لتقليل تأثير الحالة الغير متجانسة و حائط الإشارات غير المرغوب بها. هذه التقنية هي تقليص المويجة. تم مناقشة الحالات المتجانسة وغير المتجانسة والاشارات غير المرغوب بها ومقارنتها مع الحالة السابقة بدون استعمال تقليص المويجة والحصول على ربح بنسبة الإشارة إلى الضوضاء بمقدار 2.6dB لتحقيق نفس احتمالية الكشف.

1. Introduction

The goal of CFAR constant false alarm rate algorithms is to set thresholds high enough to limit false alarms to a tolerable rate. When received echo reached to CFAR processor it's entrance to shift register called CFAR window that contain number of cells [1]. The middle cell of CFAR window is contained the target which called "cell under test" (CUT) and other cells that surrounding (CUT) contain information about target environment and there are called "reference cells" in either homogenous or non-homogenous environments [2]. Since the clutter added to noise power is not refer to any given location, a fix threshold detection scheme cannot be applied to the echo in individual range cells if the false alarm rate is to be controlled. This set the threshold based on local information of total noise power [3].

The most basic forms of the adaptive detection processors are well-known mean level detector such as in 1998 a new adaptive coherent CFAR wavelet detector which can be used as an additional independent detector for effective CFAR detection of point targets [4], in 2005 another preprocessing approach based on a non-linear compressing filter to reduce the noise effect [5], in 2007 a CFAR detector based on de-noising via wavelet shrinkage [6], in 2008 improved the switching CFAR (S-CFAR) in order to fix the false alarm rate (FAR) not only in the homogenous environment with thermal noise but also in a non-homogenous environment. This CFAR is known as Improved Switching CFAR (IS-CFAR) [7] and in 2013 a new composite of CFAR processor also known as Improved switching CFAR (IS-CFAR) but it is different from first IS-CFAR in 2008 because it have a new algorithm [8].

The word wavelet stands for small wave. Wavelets have been introduced for representation of functions in a more efficient manner than Fourier series. Wavelets are generated from one single function, called mother wavelet, by translation and dilation. Wavelets have found applications in data compression, noise removal, pattern recognition, fast computation etc. [9].

The wavelet transform is really a family of transforms that satisfy specific conditions. The wavelet transform can be described as a transform that has basis functions that are shifted and expanded versions of themselves, because of this, the wavelet transform contain both frequency information and time information.

The major goal of noise reduction is to restore the original signals from noisy environments. The wavelet transform has been shown to be a powerful tool for noise reduction due to its capability of sparse representation1. Wavelet based scheme via hard shrinkage and soft shrinkage [10].

2. Improved Switching CFAR (IS-CFAR)

In IS-CFAR method, the reference cells is divided into the leading window (called A for simplification) and lagging windows (called B for simplification). Each of windows A and B contained from N/2 reference cells, the block diagram of IS-CFAR is illustrated in **Figure (1)** [8].

The reference cells in window A and B are partitioned into two sets $S_{0,A/B}$ and $S_{1,A/B}$, respectively by comparing leading window A with the result from multiplication of the Cell Under Test (CUT) with scale factor (α) if the leading window A more than the result from multiplication save $X_{K,A}$ in $S_{0,A}$ else neglect it and if the length of $S_{0,A}$ called $n_{0,A}$ and same thing for lagging window B to generate $S_{0,B}$ and $n_{0,B}$ [8].

Where $S_{0,A/B}$ denotes $S_{0,A}$ or $S_{0,B}$, $S_{1,A/B}$ denotes $S_{1,A}$ or $S_{1,B}$, $X_{k,A/B}$ denotes $X_{k,A}$ or $X_{k,B}$ for simplification. After all of the reference cells in window A and B have been compared with αX_0, let $n_{0,A}$ and $n_{0,B}$ denote the numbers of cells contained in $S_{0,A}$ and $S_{0,B}$, respectively [8].

In next step threshold will be calculated according to block diagram in **Figure (1)** then compare with cell under test (CUT) to make decision.

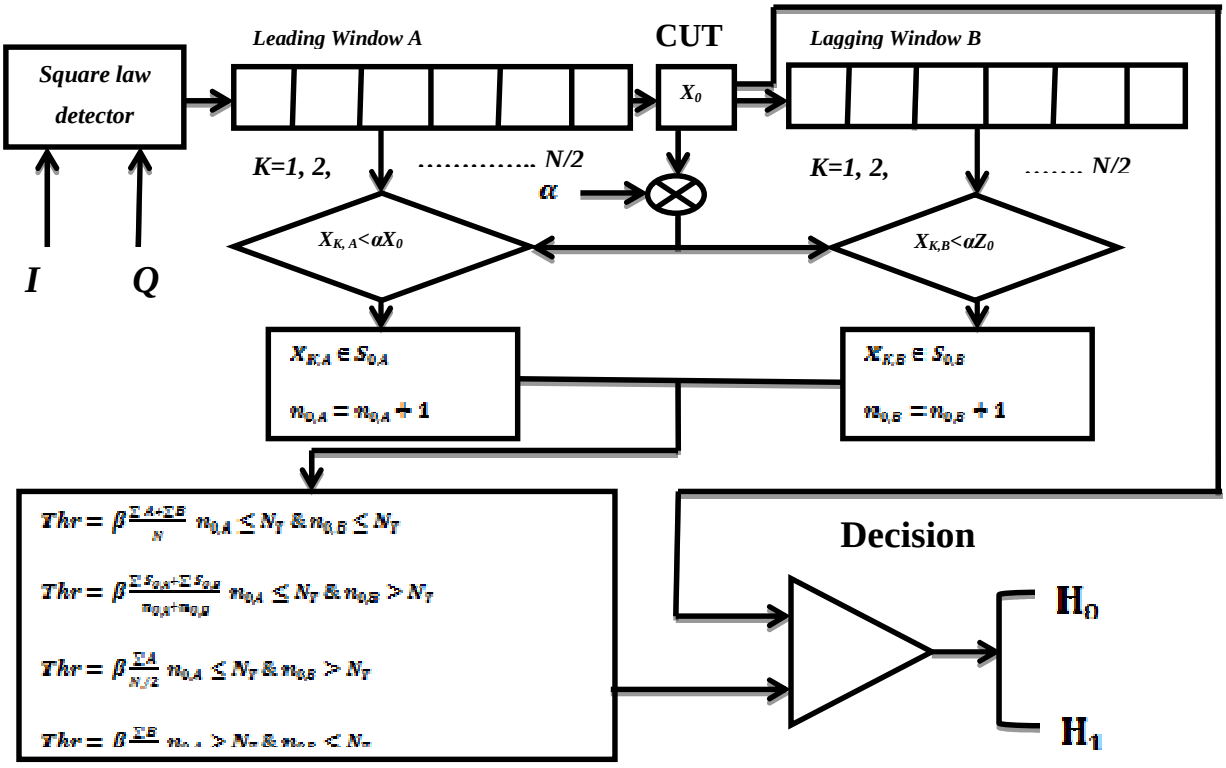

Fig .(1). Block diagram of (IS-CFAR)

As described earlier, non-homogeneities are the main problem of CFAR detection. In CFAR detection, two kinds of non-homogeneities, i.e. interfering targets and clutter-edge are considered. Interfering targets are strong signals related to targets appeared in reference cells and cause an incorrect estimation of the level of the noise in CFAR processor and so decrease the probability of detection. Clutter-edge is the situation in which power of the clutter in reference cells changes from one level to another level, instantaneously. Also, it causes an incorrect estimation of the level of the noise and changes the probability of false alarm [6].

In this paper a new tool of CFAR detector to reduce the non-homogenous effect on probability of detection and to reduce clutter wall effect.

To plot probability of detection in non-homogenous environment the equation (1) will used, probability of detection in homogenous environment is obtained by set $M_a = 0$ & $M_b = 0$ & $\sigma_I = 0$. The probability of false alarm is obtained by set $M_a = 0$ & $M_b = 0$ & $\sigma_I = 0$ & $\sigma_S = 0$ [8].

$$P_d = \frac{1}{1+\sigma_S}\sum_{n_{0,A}=0}^{N_T}\sum_{n_{0,B}=0}^{N_T}\sum_{m=M_{0,A}}^{\min(M_A,n_{0,A})}\sum_{n=M_{0,B}}^{\min(M_B,n_{0,B})}\binom{(N/2)-M_A}{n_{0,A}-m}\binom{(N/2)-M_B}{n_{0,B}-n}\times \binom{M_A}{m}\binom{M_B}{n}\sum_{b=0}^{u-v}\sum_{c=0}^{v}\frac{(-1)^{b+c}\binom{u-v}{b}\binom{v}{c}}{(1+\sigma_I)^M}W_1$$

$$+\frac{1}{1+\sigma_S}\sum_{n_{0,A}=N_T+1}^{N/2}\sum_{n_{0,B}=N_T+1}^{N/2}\sum_{m=M_{0,A}}^{\min(M_A,n_{0,A})}\sum_{n=M_{0,B}}^{\min(M_B,n_{0,B})}\binom{(N/2)-M_A}{n_{0,A}-m}\binom{(N/2)-M_B}{n_{0,B}-n}\times \binom{M_A}{m}\binom{M_B}{n}\sum_{b=0}^{u-v}\sum_{c=0}^{v}\frac{(-1)^{b+c}\binom{u-v}{b}\binom{v}{c}}{(1+\sigma_I)^v}W_2$$

$$+\frac{1}{1+\sigma_S}\sum_{n_{0,A}=0}^{N_T}\sum_{n_{0,B}=N_T+1}^{N/2}\sum_{m=M_{0,A}}^{\min(M_A,n_{0,A})}\sum_{n=M_{0,B}}^{\min(M_B,n_{0,B})}\binom{(N/2)-M_A}{n_{0,A}-m}\binom{(N/2)-M_B}{n_{0,B}-n}\times \sum_{d=0}^{n_{0,B}-n}\sum_{f=0}^{n}\sum_{b=0}^{n_{0,A}-m}\sum_{c=0}^{m}\frac{(-1)^{d+f+b+c}\binom{n_{0,B}-n}{d}\binom{n}{f}\binom{n_{0,A}-m}{b}\binom{m}{c}}{(1+\sigma_I)^{M_A}}\binom{M_A}{m}\binom{M_B}{n}W_3$$

$$+\frac{1}{1+\sigma_S}\sum_{n_{0,A}=N_T+1}^{N/2}\sum_{n_{0,B}=0}^{N_T}\sum_{m=M_{0,A}}^{\min(M_A,n_{0,A})}\sum_{n=M_{0,B}}^{\min(M_B,n_{0,B})}\binom{(N/2)-M_A}{n_{0,A}-m}\binom{(N/2)-M_B}{n_{0,B}-n}\times \binom{M_A}{m}\binom{M_B}{n}\sum_{d=0}^{n_{0,A}-m}\sum_{f=0}^{n}\sum_{b=0}^{n_{0,B}-n}\sum_{c=0}^{m}\frac{(-1)^{d+f+b+c}\binom{n_{0,B}-n}{d}\binom{n}{f}\binom{n_{0,A}-m}{b}\binom{m}{c}}{(1+\sigma_I)^{M_B}}W_4 \quad \ldots\ldots\ldots \textbf{(1)}$$

Where W_1, W_2, W_3 and W_4 is obtained from equations (2), (3), (4) and (5).

$$W_1 = \frac{\varsigma^N}{[\rho_1+\varsigma+(1+\sigma)^{-1}]^N[\rho_1+(1+\sigma)^{-1}]}\left[1-\frac{\varsigma\sigma_I}{(1+\sigma_I)(\rho_1+\varsigma+(1+\sigma)^{-1})}\right]^{-M} \quad \ldots\ldots\ldots\ldots\ldots \textbf{(2)}$$

$$W_2 = \frac{\varepsilon^u}{[\rho_2+\varepsilon+(1+\sigma)^{-1}]^u[\rho_2+(1+\sigma)^{-1}]}\left[1-\frac{\varepsilon\sigma_I}{(1+\sigma_I)(\rho_2+\varepsilon+(1+\sigma)^{-1})}\right]^{-v} \quad \ldots\ldots\ldots\ldots\ldots\ldots \textbf{(3)}$$

$$W_3 = \frac{\varrho^{N/2}}{[\rho_3+\varrho+(1+\sigma)^{-1}]^{N/2}[\rho_3+(1+\sigma)^{-1}]}\left[1-\frac{\varrho\sigma_I}{(1+\sigma_I)(\rho_3+\varrho+(1+\sigma)^{-1})}\right]^{-M_A} \quad \ldots\ldots\ldots\ldots\ldots \textbf{(4)}$$

$$W_4 = \frac{\Psi^{N/2}}{[\rho_4+\Psi+(1+\sigma)^{-1}]^{N/2}[\rho_4+(1+\sigma)^{-1}]}\left[1-\frac{\Psi\sigma_I}{(1+\sigma_I)(\rho_4+\Psi+(1+\sigma)^{-1})}\right]^{-M_B} \quad \ldots\ldots\ldots\ldots\ldots\ldots \textbf{(5)}$$

To determine W_1, W_2, W_3 and W_4 ρ_1, ρ_2, ρ_3 and ρ_4 must calculate from following equations.

$$\rho_1 = \rho_2 = \alpha\left[N - M - u + b + v + \frac{M+c-v}{1+\sigma_I}\right] \quad \ldots\ldots\ldots\ldots\ldots\ldots\ldots \textbf{(6)}$$

$$\rho_3 = \rho_4 = \alpha\left[d + N - (M_A + M_B) - (n_{0,A} + n_{0,B}) + b + m + n + \frac{c+f+(M_A+M_B)-(m+n)}{1+\sigma_I}\right] \quad \text{(7)}$$

$$\zeta = \frac{N}{\beta} - \alpha(N - u + b + c) \quad \text{(8)}$$

$$\varepsilon = \frac{u}{\beta} - \alpha(b + c) \quad \text{(9)}$$

$$\varrho = \frac{N/2}{\beta} - \alpha(N/2 - n_{0,A} + b + c) \quad \text{(10)}$$

$$\Psi = \frac{N/2}{\beta}\alpha\left(N/2 - n_{0,B} + b + c\right) \quad \text{(11)}$$

$$M_{0,A} = \max(0, n_{0,A} - N + M_A) \quad \text{(12)}$$

$$M_{0,B} = \max(0, n_{0,B} - N + M_B) \quad \text{(13)}$$

$$M = M_A + M_B \quad \text{(14)}$$

$$u = n_{0,A} + n_{0,B} \quad \text{(15)}$$

$$v = m + n \quad \text{(16)}$$

Where ζ, ε, ψ and φ must be greater than zero and the negative number is neglected, $n_{0,A}, n_{0,B}, m, n, d, c, b, f$ is counters of sum.

σ_S : Signal to noise ratio

σ_I : Interference to noise ratio

N_T : Threshold integer

M_A : Number of interference target in leading window A

M_B : Number of interference target in leading window B

$n_{0,A}$: Number of reference cells stored in $S_{0,A}$

$n_{0,B}$: Number of reference cells stored in $S_{0,B}$

3. Improving IS-CFAR using wavelet de-noising (I^2S-CFAR)

Wavelet shrinkage is discovered by Donoho and Johnstone to remove the noise that comes from weather.

Wavelet de-noising block put on input Y for estimation of probability of detection for given P_{fa} using wavelet de-noising and before square law detector on [I & Q]. First operator in de-noising block is discrete wavelet decomposition. The wavelet family, which is used in this algorithm, can be selected from Symlet, Coiflet, Daubechies or other families. The second operator is to choose the threshold of de-noising which shrinks wavelet coefficients, there is classified in to two main types hard and soft threshold. We used soft threshold that classified to this types Universal threshold, Stein's Unbiased Risk Estimation (SURE) and Block threshold (BT).

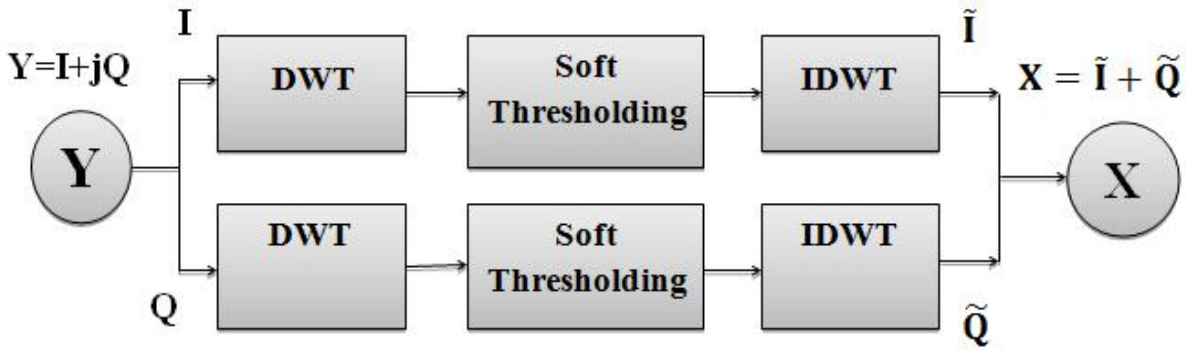

Fig .(2). Wavelet De-noising Block Diagram

At the end the third operator is used to reconstruct the signal and use all performance of first operator as shown in **Figure (2).**

The block diagram, which shows the implementation of wavelet block with IS-CFAR, is depicted in **Figure (3).** The basic idea of algorithm is that its first stage the free signal X is made from de-noising block that contain only target is subtracted from the original signal (Y-X to get Z) in next step the result from subtract (Z) applied to square law detector (SLD).

Wavelet family "dB2" is used for signal decomposition, because of less computational complexity due to its short impulse response in order to separate the signal from local noise phenomena. In this study, four levels of decomposition for DWT are used because this is very enough to give an accurate result. SURE shrinkage method is used for simplification if compare it with other methods and it gives a accurate result. Flow chart of drawing probability of detection in I^2S-CFAR shows in **Figure (4).**

CUT can be selected from de-noised signal (X) or original signal (Y) but because of some information loss in de-noising algorithm, it is recommended to use the original signal (Y), as CUT.

Therefore, for improving of IS-CFAR using wavelet de-noising (I^2S-CFAR) the scaling factor β is different from the scaling factor of normal IS-CFAR to get the same probability of false alarm. Scaling factor β depends on some parameters such as:

- wavelet family
- levels of signal decomposition
- number of reference cells
- method of de-noising
- statistical parameters of noise
- probability of false alarm
- threshold integer (N_T)
- The parameter (α)

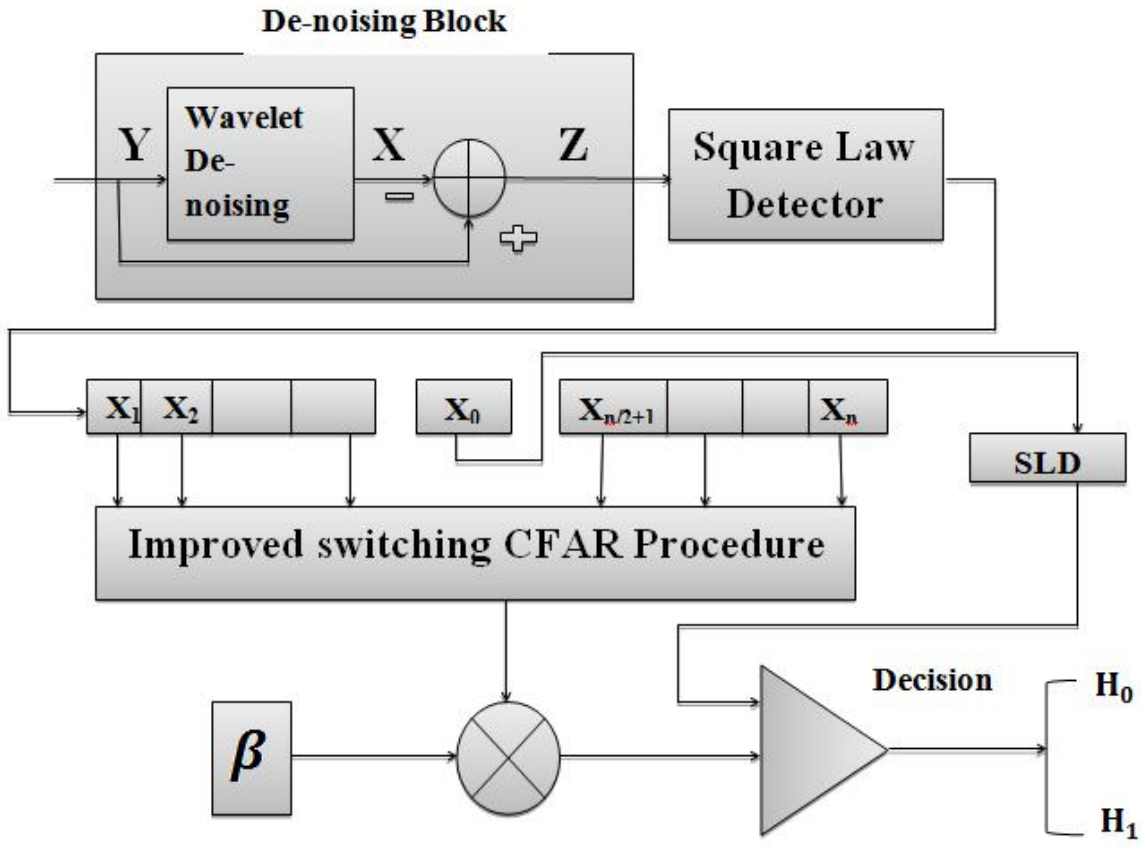

Fig .(3) I^{2}S-CFAR Block diagram

4. Estimation of Probability of Detection Algorithm for given PFA using Wavelet de-noising

4.1. Step -1-

The value of all CFAR parameters can be calculated from the basic criteria of IS-CFAR. Probability of false alarm, alpha and substitute vector from Beta values are assumed to calculate the value of Beta in order to draw curve between Beta and probability of false alarm.

Varying values of β in the range [14, 26], and using equation (1) for IS-CFAR, we obtained the curve which relates the two parameters. The required values of β are Extracted according to the correspondence values of P_{fa} [10^{-5}, 10^{-6}] from the probability of false alarm curve.

4.2. Step -2-

In this step a simulation is made using trial and error program to obtain the values of β which corresponds to the obtained value of β from step -1-.

The reference cells will occupied by White Addition Gaussian Noise (AWGN) which contain real named I channel and imaginary part named Q channel, while the distribution of signal in cut will be exponential distribution for swerling II or chi-square for swerling III with noise power. The number of iteration equal to $1/P_{fa}$.

Every row in array acts as a reference window and the threshold (Thr) can be determined for every row by applying the IS-CFAR statistic to get (I^2S-CFAR) and compare it with cell under test (CUT) (X_0) if cell under test (CUT) is more than threshold choose hypothesis H_1 and if else choose hypothesis H_0.

$$X_0 \underset{H_1}{\overset{H_0}{\lessgtr}} Thr \quad \text{..... (17)}$$

The summation hypothesis H_1 is found for all iterations and divide the summation on number of iteration to get the probability of false alarm.

The obtained result contain values of $P_{fa} = 0$, which were eliminated, and the rest value of P_{fa} which correspond to required value [10^{-5}, 10^{-6}] were found for a range of β, which are equal to β calculated from step -1- or less.

4.3. Step -3-

In this step the wavelet block is combined with the IS-CFAR block. The input noise is taken from step -2- limited for the part of β calculated from step -1- or less.

The noise array is entered to de-noising block to subtract its output from the original signal. Now every row in the result from subtracting acts as a CFAR window.

The threshold (Thr) can be determined for every row by applying the IS-CFAR statistic to get (I^2S-CFAR) and to be compared with cell under test (CUT) (X_0). If cell under test (CUT) is more than threshold choosing hypothesis H_1, and if none choose hypothesis H_0.

The summation hypothesis H_1 is found for all iterations and the summation is divided on number of iterations to get the probability of false alarm.

The results of simulation give a new range of β with respect to the required value of P_{fa}. In correspondence with step -2-, the max value of β is taken.

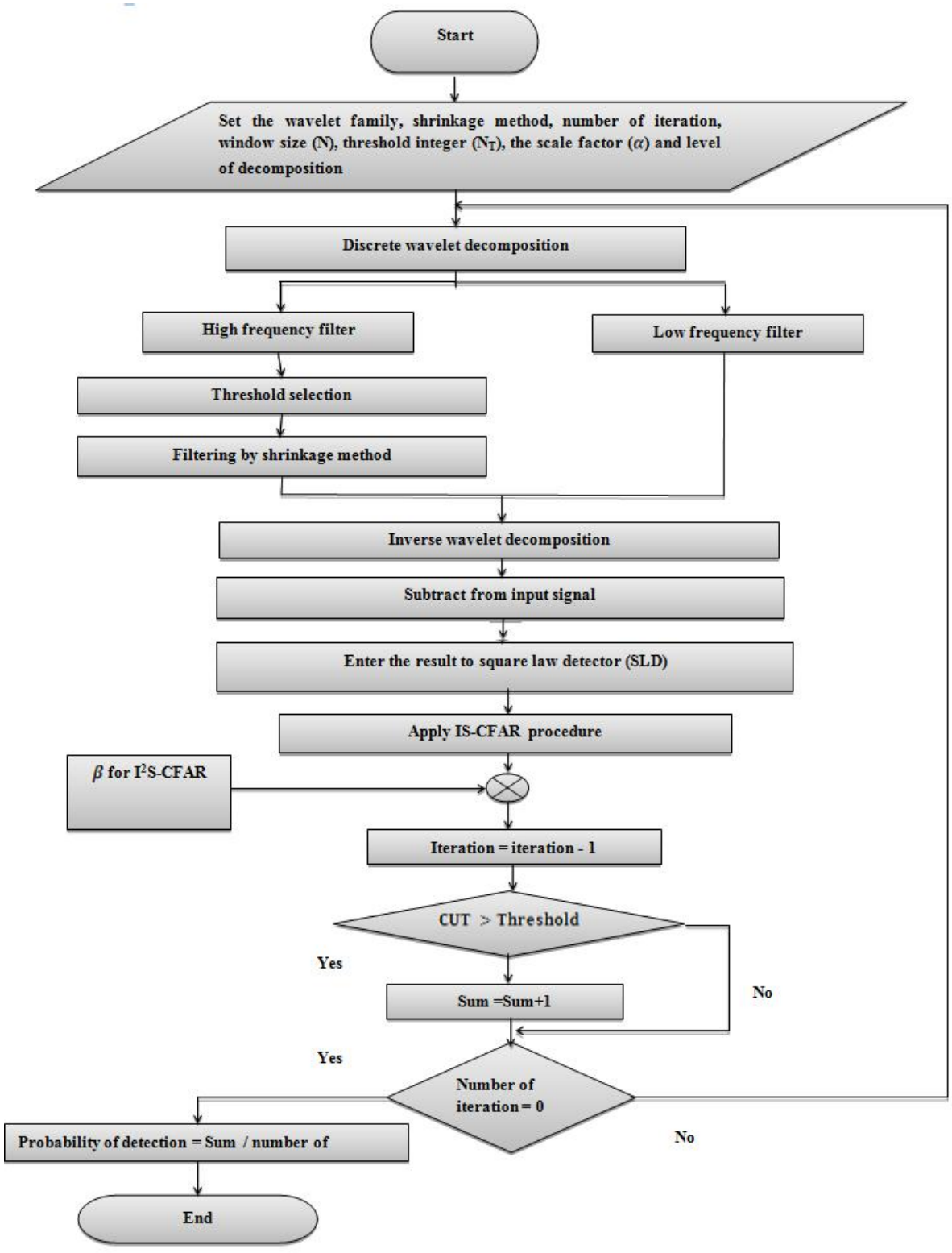

Fig .(4) Flow Chart of improving of IS-CFAR using wavelet de-noising

4.4. Step -4-

Plot curve between probability of detection and signal to noise ratio (SNR) in case of wavelet de-noising by using alpha & beta from step -3- and the same algorithm of probability of false alarm in case (I^2-SCFAR) except for using signal power instead of noise power to determine probability of detection in homogenous environment.

To draw probability of detection in non-homogenous environment same algorithm in homogenous environment is used except for replacing (M) columns from input array by other columns which have same distribution of cell under test (CUT) (M is number of interference target). Flow chart of drawing probability of detection in I^2S-CFAR is shown in **Figure (4).**

5. Simulation Results and Discussions

The obtained relation between probability of false alarm and β is illustrated in **Figure (5).**

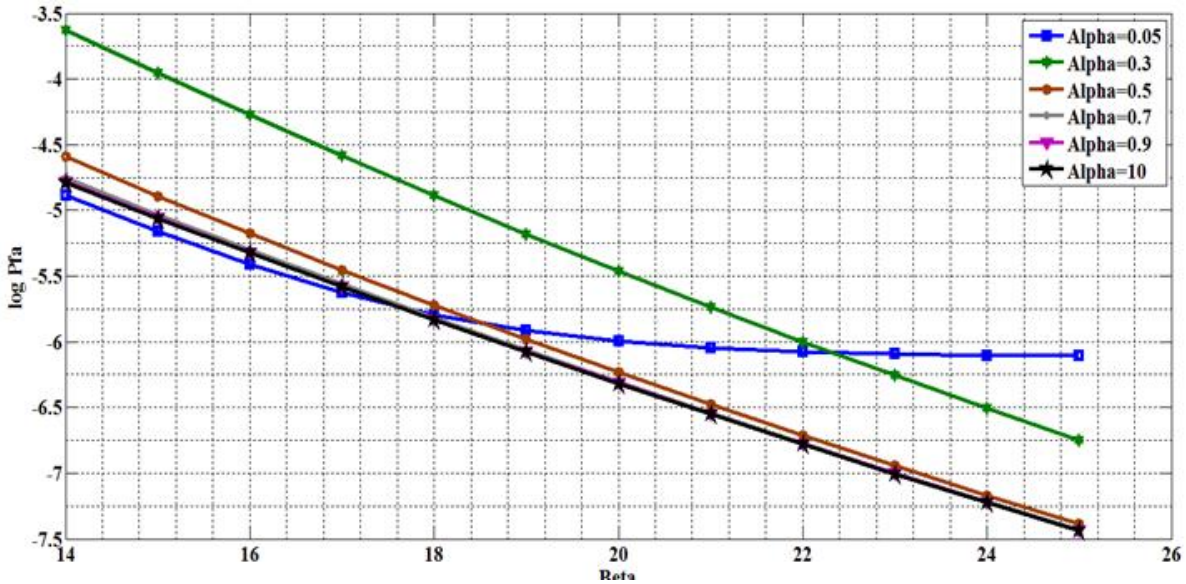

Fig .(5) Probability of false alarm of IS-CFAR Swerling II

If the number of reference cells (N = 24) and the threshold integer (N_T = 7). **Table (1)** depicted the drive values of probability of false alarm $P_{fa} = 10^{-6}$ with respect to β in range of α are between (0.05 and 10) for IS-CFAR without using wavelet de-noising.

Table 1 Values of α and β at $P_{fa} = 10^{-6}$, N=24, N_T=7

α	0.05	0.3	0.5	0.7	0.9	10
β	20.03	22	19.8	18.74	18.69	18.69

Tables (2) represent the values of α and β for improving IS-CFAR using wavelet de-noising (I^2S-CFAR) at probability of false alarm $P_{fa} = 10^{-6}$.

Table 2 Values of α and β at $P_{fa} = 10^{-6}$, N=24, N_T=7

α	0.05	0.3	0.5	0.7	0.9	10
β	41.98	22.84	22.46	23.62	19.53	20.4

Detection characteristics curves in homogenous case, swerling II case and multi alpha can be plotted using **Table (2)** for $P_{fa} = 10^{-6}$ as show in **Figure (6).**

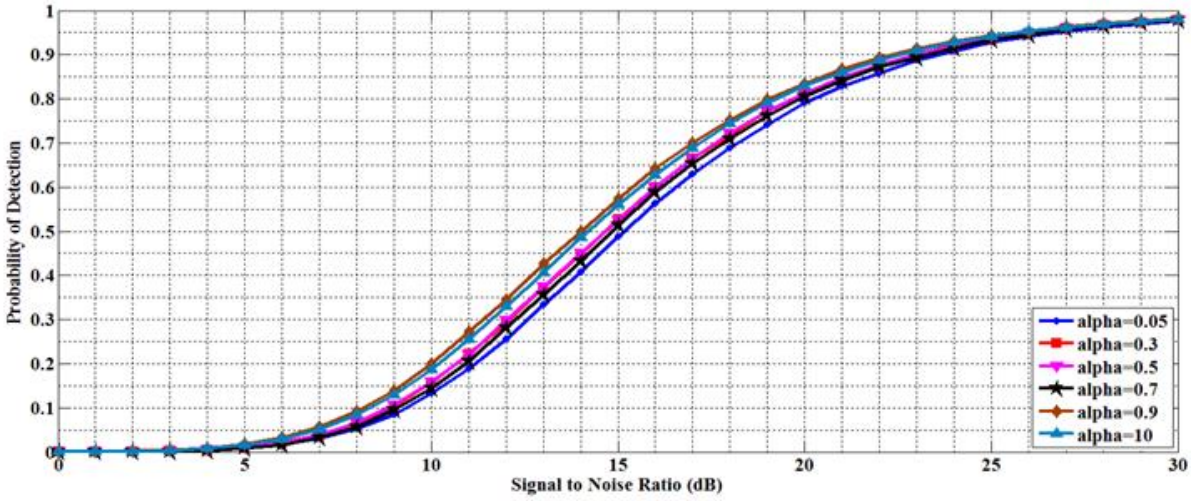

Fig .(6) I^2S-CFAR Probability of Detection Homogeneous Environment Swerling case II and $P_{fa} = 10^{-6}$

The max probability of detection is obtained for α = 0.9 in swerling case II at $P_{fa} = 10^{-6}$.

Figure (7) show the probability of detection curves are plotted for IS-CFAR and I^2S-CFAR at $P_{fa} = 10^{-6}$ in Homogenous Environment threshold integer (N_T=7), optimum alpha for I^2S-CFAR (α =0.9), scale factor for IS-CFAR (α =0.05) and swerling case II radar target.

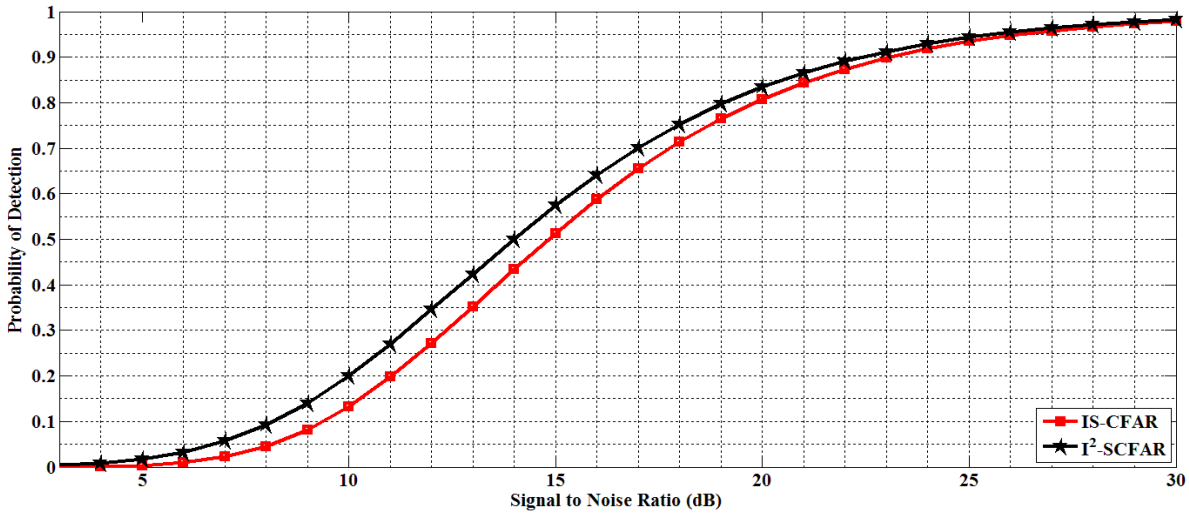

Fig .(7) Comparison of detection characteristics in Homogenous Environment

From **Figure (7),** the probability of detection is equal to the range [0.5, 0.7] when the signal to noise ratio (SNR) in the range [14dB, 17dB] at $P_{fa} = 10^{-6}$ and optimum alpha for I^{2}S-CFAR. The probability of detection is equal to the range [0.5, 0.7] when the signal to noise ratio (SNR) in the range [14.8dB, 17.75dB] for IS-CFAR.

It shows that IS-CFAR and I^{2}S-CFAR have nearly same performance in homogeneous scenario.

Figure (8) show the probability of detection curves are plotted for IS-CFAR and I^{2}S-CFAR at $P_{fa} = 10^{-6}$ in Non-Homogenous Environment, threshold integer (N_T=7), optimum alpha for I^{2}S-CFAR (α =0.9), scale factor for IS-CFAR (α =0.05), and (one interference target in leading window (A) and two interference target in lagging window (B) (M_a = 1 & M_b = 2)).

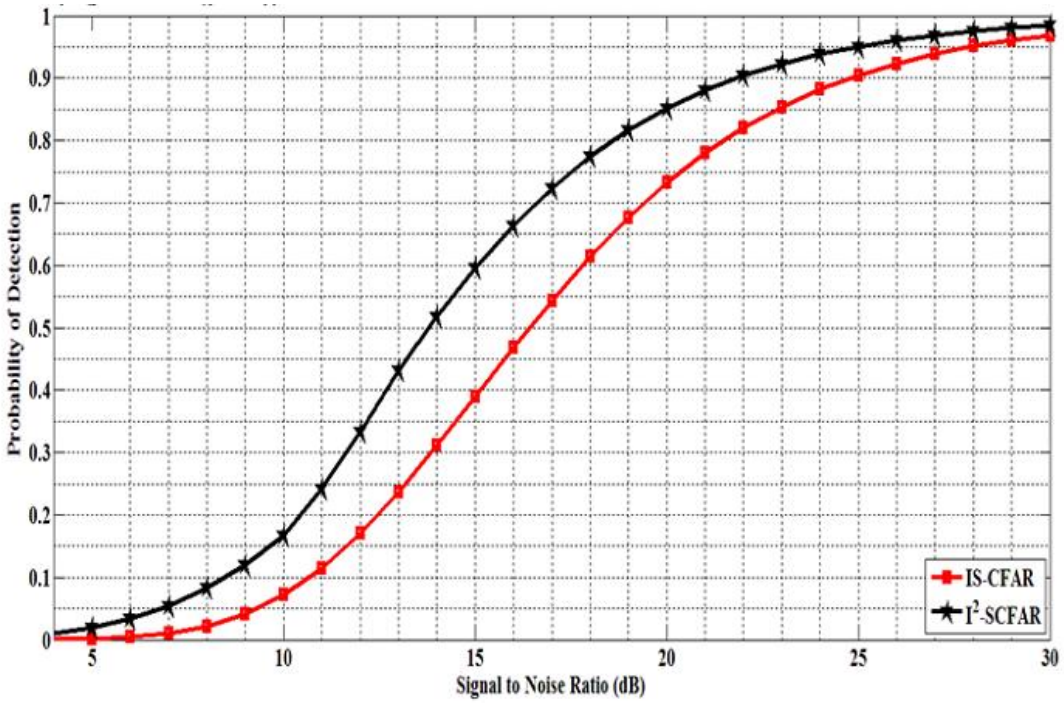

Fig .(8). Comparison of detection characteristics in Non-Homogenous Environment

From **Figure (8),** the probability of detection is equal to the range [0.5, 0.7] when the signal to noise ratio (SNR) in the range [13.8dB, 16.6dB] at $P_{fa} = 10^{-6}$, (no interference target in leading window (A) and one interference target in lagging window (B) ($M_a = 0$ & $M_b = 1$)) and optimum alpha for I^{2}S-CFAR. The probability of detection is equal to the range [0.5, 0.7] when the signal to noise ratio (SNR) in the range [16.41dB, 19.41dB] for IS-CFAR.

Figure (9) show detection characteristics in clutter wall on this performance alpha (α =0.05) for IS-CFAR, threshold integer (N_T=7), optimum alpha for I^{2}S-CFAR (α =0.9) signal to noise ratio (SNR = 15dB) and clutter to noise ratio (CNR = 10dB).

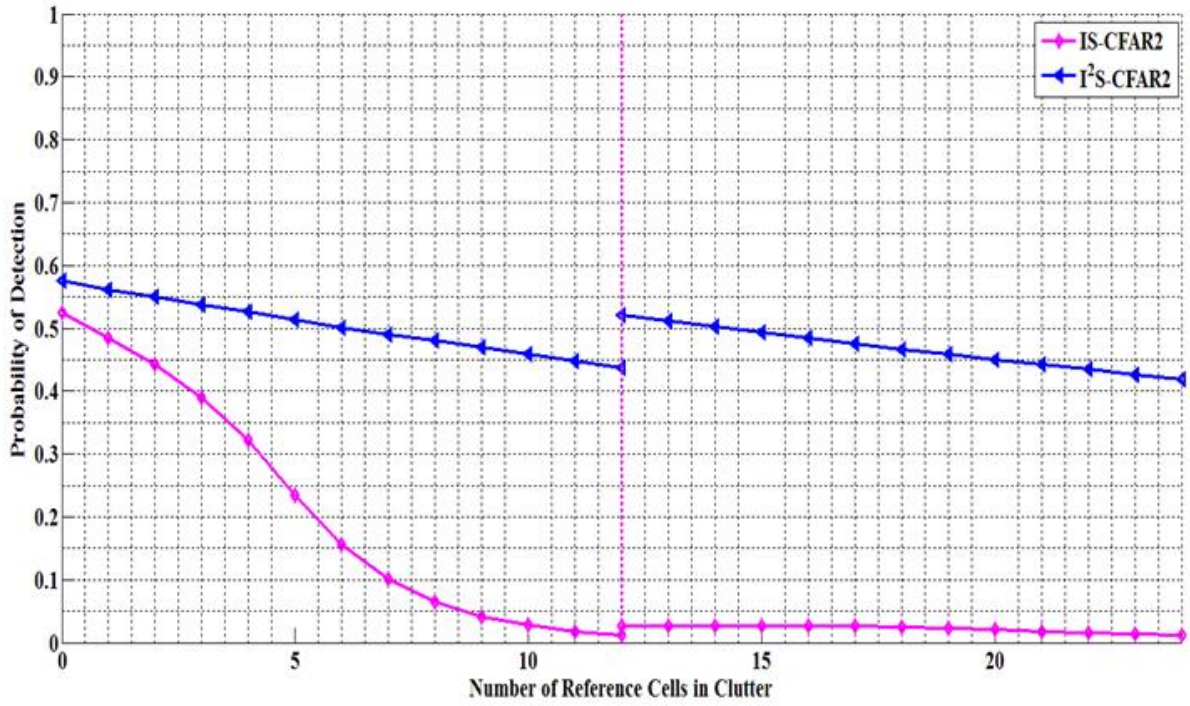

Fig .(9) Comparison of detection characteristics in clutter wall

As shown from **Figure (9)** a less degradation is noticed, the range of probability of detection fluctuation is kept in certain range about (0.575-0.42) for $P_{fa} = 10^{-6}$ from before clutter wall to after it for I^{2}S-CFAR as a compared with IS-CFAR that has the range of probability of detection fluctuation about (0.525-0.01).

The variation of slope curve in **Figure (9)** when the number of reference cells equal (N/2), is due to that the clutter to noise ratio enters to the cell under test (CUT)

The degradation in probability of detection can be attributed to a masking effect by the clutter region before the clutter wall. The decrease in probability of detection after the clutter wall can be accounted by the clutter to noise ratio (CNR).

6. Conclusions

1. For homogenous case using wavelet de-noising for IS-CFAR with given probability of false alarm, I^2S-CFAR1, $P_{fa} = 10^{-6}$ and swerling case II to ensure the probability of detection is equal to the range [0.5, 0.7] when the signal to noise ratio (SNR) in the range [14dB, 17dB]. With respect to IS-CFAR without using wavelet de-noising the probability of detection is equal to the range [0.5, 0.7] when the signal to noise ratio (SNR) in the range [14.8dB, 17.75dB].
2. for non-homogenous case using wavelet de-noising for IS-CFAR with given probability of false alarm, I^2S-CFAR, $P_{fa} = 10^{-6}$ and swerling case II to ensure the probability of detection is equal to the range [0.5, 0.7] when the signal to noise ratio (SNR) in the range [13.8dB, 16.6dB] at (M=3). With respect to IS-CFAR without using wavelet de-noising the probability of detection is equal to the range [0.5, 0.7] when the signal to noise ratio (SNR) in the range [16.41.6dB, 19.41dB] at (M=3).
3. For clutter wall case Improving IS-CFAR using wavelet de-noising for I^2S-CFAR SWII, $P_{fa} = 10^{-6}$, SNR=15dB, CNR=10dB, the range of probability of detection fluctuation is kept in certain range about (0.575-0.42) for from before clutter wall to after it but for Improving IS-CFAR without using wavelet de-noising the range of probability of detection fluctuation influence a large degradation in certain range about (0.525-0.01) for from before clutter wall to after it.
4. Implementation of wavelet to improve IS-CFAR has disadvantages related with increase complexity of circuit and increase time processing.

7. References

1. **James J. Jen "A Study of CFAR Implementation Cost and Performance Tradeoffs in Heterogeneous Environments", A master Thesis Presented to the Faculty of California State Polytechnic University, Pomona, 2011.**
2. **M. B. El Mashade " Analysis of CFAR Detection of Fluctuating Targets" Electrical Engineering Department Faculty of Engineering Al Azhar University Nasr City, Cairo, Egypt Progress In Electromagnetics Research C, Vol. 2, 65–94, 2008.**
3. **Gandhi, P.P., Kassam, S.A.: "Analysis of CFAR Processors in Non-Homogenous Background", IEEE Transactions on Aerospace and Electronic Systems, Vol.24, No.4, pp. 427-445, July 1988. .(IVSL)**
4. **G.A. Lampropoulosa, G. Giglia, A. ajjb and M. Rey "A New Adaptive Coherent CFAR Wavelet Detector" SPIE 1St. Clair Avenue West, Suite 1103 Toronto, Ontario, CANADA Vol. 3491 pp.1010-1016 1998.**

5. **Z. Messalil, M. SahmoudP and F. Soltani "Robust Detection of Distributed CA-CFAR in Presence of Extraneous Targets and Non-Gaussian Clutter" IEEE Electronic Departement, Constantine University, Algerie 2 TSI, Telecom-Paris, 37-39, rue Dareau, 75014 Paris, France pp.547-550, 2005. .(IVSL)**
6. **M. Alamdari, M. Modarres-Hashemi "An Improved CFAR Detector Using Wavelet Shrinkage in Multiple Target Environments" IEEE Department of Electrical and Computer Engineering, Isfahan University of Technology, Isfahan, Iran 2007. .(IVSL)**
7. **Saeed Erfanian1, Vahid T. Vakili "Analysis of Improved Switching CFAR in the Presence of Clutter and Multiple Targets" IEEE Electrical Engineering Department, Iran University of Science & Technology (IUST) Narmak 16846, Tehran, Iran PP.257-260, 2008. .(IVSL)**
8. **Renli Zhang, WeixingSheng n, XiaofengMa "Improved switching CFAR detector for non-homogeneous environments" ScienceDirect School of Electronic and Optoelectronic Engineering, Nanjing University of Science and Technology, Nanjing 210094, China, Signal Processing volume 93 issue 1 pp.35–48 January 2013. .(IVSL)**
9. **Stephane Mallat "A Wavelet Tour of Signal Processing" 2nd edition, New York University, 1999.**
10. **Qiang Guoa, Caiming Zhanga "A noise reduction approach based on Stein's unbiased risk estimate" scienceasia School of Computer Science and Technology, Shandong University of Finance and Economics, Erhuan Dong Road, Jinan, 250014, China pp. 207–21, 2012.**